X-ray-scattering study of the cubic-to-tetragonal transition and its precursive phenomenon in V_3Si

K. Hirota, L. Rebelsky,* and G. Shirane
Department of Physics, Brookhaven National Laboratory, Upton, New York 11973
(Received 1 December 1994)

We searched for the order parameter of V_3Si below the cubic-to-tetragonal transition at $T_M \approx 21$ K. Appearance of *new* Bragg peaks at (100) and (300) reflections, which are forbidden in the cubic phase, has been confirmed below T_M, after multiple scattering was removed. Temperature dependence of the intensities indicates that the sublattice displacements are linear to the tetragonal strain as is the case with Nb_3Sn. We also found that, even above T_M, there remain intensities at (100) and (300), which gradually decrease with increasing temperature. We speculate that this is a precursor to the martensitic transition, possibly due to the covalency effect between V atoms or the anharmonicity in the softening of the zone-center phonon.

I. INTRODUCTION

Members of the $A15$ compounds (the general formula A_3B with the space group $Pm\bar{3}n$) show high superconducting transition temperatures T_C's as well as a cubic-to-tetragonal martensitic transition at T_M.[1] Our primary purpose of this work was to search for the order parameter of the martensitic transition in a prototypical system V_3Si ($T_C \approx 17$ K, $T_M \approx 21$ K), which has not been established for three decades since the transition was reported by Batterman and Barrett.[2] Yet another system of the $A15$ compound, Nb_3Sn ($T_C \approx 18$ K, $T_M \approx 50$ K),[3] has been under extensive experimental and theoretical investigations for many years. The martensitic transition of Nb_3Sn is characterized by a drastic softening of the [110] transverse acoustic (TA) phonon near the zone center,[4,5] changing a cubic phase to a slightly distorted tetragonal phase ($a/c = 1.0062$). Shirane and Axe[6] revealed appearance of *new* Bragg reflections such as (300), which are forbidden in the cubic phase, in Nb_3Sn below T_M by neutron scattering. From the intensity distribution among the new Bragg peaks, they uniquely determined that the tetragonal structure is $P4_2/mmc$ with Nb displacements of 0.016(3) Å at 4 K in a pattern identical to the eigenvectors of the $\Gamma_{12}(+)$ optic-phonon mode in the cubic phase (see Fig. 1). They also found that the internal sublattice displacement δ is proportional to the spontaneous tetragonal strain ($a/c - 1$). This discovery in Nb_3Sn has established that the appropriate order parameter is either the tetragonal strain or the sublattice distortion, which are linearly related.

V_3Si has been studied even more exhaustively than Nb_3Sn. Batterman and Barrett[7] carried out detailed x-ray studies and clarified the cubic-to-tetragonal transformation at T_M with distortion progressively increasing from unity to $c/a = 1.0024$. They pointed out that some characteristics of the martensitic transition vary from sample to sample. A *well-behaved* sample exhibited a smooth but rapid change at $T_M = 21.0 \pm 0.5$ K in the c/a ratio without showing any precursive shift in the lattice constant above T_M. In another sample they studied, however, the c parameter decreased rapidly above 17 K along a curve which extrapolates to $T_M = 23$ K. There is an inflection point in the curve at 21 K and the crystal remained tetragonal up to approximately 27 K. They also reported a sample which showed the c/a ratio half as large as the value of well-behaved samples and a sample which did not transform at all. The sample dependence of T_M has been systematically studied by Khlopkin.[8] He reported that T_M falls off monotonically with increasing defect concentration which was estimated by measuring a ratio of the resistivity at 300 K and at 18 K. His specific heat measurements also showed broadening of the transition similar to that of the lattice constant, which he ascribed to an inhomogeneity of the samples. A similar broad transition was reported in x-ray measurements as

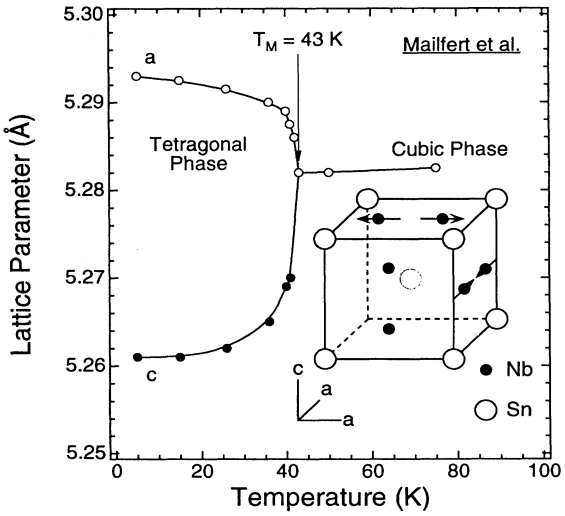

FIG. 1. Temperature dependence of the lattice parameter of Nb_3Sn after Ref. 3. The inset shows a Nb-sublattice atomic shift below T_M, corresponding to the $\Gamma_{12}(+)$ mode.

a precursive broadening of the Bragg peak width as the transition is approached from above.[9,10] After etching, a drastic reduction of the peak broadening was seen, which was attributed to decrease of surface strain.

Although neutron-scattering experiments[11] revealed a remarkable softening of the [110] TA phonon in V_3Si as in Nb_3Sn, the new Bragg reflections corresponding to the order parameter have not been detected yet. A small coherent scattering of V (-0.05×10^{-12} cm) compared with 0.42 for Si and 0.69 for Nb makes a neutron-scattering study extremely difficult. At the same time, a large incoherent scattering of V creates a large background and absorption. Smaller tetragonal distortion in V_3Si than that of Nb_3Sn increases the difficulty even more because the intensity of a new Bragg reflection is expected to be proportional to the *square* of the tetragonal strain as shown in Nb_3Sn.[6] Another way to measure the new Bragg reflections is an x-ray-scattering measurement. Perel, Batterman, and Blount[12] indeed tried to clarify the tetragonal structure of V_3Si but did not succeed. Intensities of the new Bragg reflections of V_3Si are estimated at too small (typically 10^{-6}–10^{-8} of the fundamental peak intensities) to be detected with x rays from an ordinary rotating anode. Moreover, multiple scattering appearing at the forbidden reflections easily overrides a weak new Bragg peak. Progress of utilizing synchrotron radiation for x-ray scattering has finally made it possible to observe new Bragg reflections in V_3Si. The high luminescence gives a detectable intensity for the new Bragg peak. Both a well-collimated beam resulting in a good resolution and a variation of the incident energy help the elimination of multiple scattering. In the present paper, we report on the new Bragg peaks at forbidden reflections (100) and (300) and their temperature dependence. We compare the new Bragg peak intensities and the tetragonal strain to establish the order parameter.

In the course of studying the new Bragg reflections, we found a very interesting phenomenon: Even above T_M, there remain finite intensities at (100) and (300), which are supposed to be forbidden in the cubic phase. These intensities gradually increase with decreasing temperature from room temperature to T_M, indicating a precursive phenomenon closely related to the martensitic transition. Although these "residual" intensities were rather surprising to us, the existence of other forbidden reflections in V_3Si have been investigated in the past from a different perspective. Borie[13] proposed a theoretical model for thermally excited forbidden reflections in V_3Si and several experiments followed.[14–16] We will come back to this aspect in our discussion.

II. EXPERIMENTAL DETAILS

Two single-crystal samples of V_3Si were examined. Sample 1 has a right cylindrical shape ($r = 2$ mm, $h = 4$ mm) with ⟨100⟩ parallel to the cylinder axis. Sample 2, which was used in Ref. 11, has a parallelepiped shape with dimensions $10\times7\times5$ mm^3, in which each face is perpendicular to one of ⟨100⟩ directions. The (100) faces of both crystals were first prepared by mechanical polishing and then, before starting the experiments, etched for 5 min with the etchant consist of H_2O, concentrated HF, and 30% H_2O_2 in the proportions 4:1:1, as employed in Ref. 10. This procedure produced a surface with a mosaic width of 0.046° full width at half maximum (FWHM), one-third of that before the etching, for sample 1 and 0.022° FWHM for sample 2. The lattice parameter at room temperature is 4.72 Å.

X-ray experiments were performed at Brookhaven National Laboratory in the National Synchrotron Light Source on a beam line X22C, equipped with a mirror to cut off the incident energy higher than 11.5 keV, a variable double-crystal Ge(111) monochromator, and a Ge(111) analyzer in the vertical scattering geometry. This configuration leaves practically no $\lambda/2$ contamination for the incident energy higher than 5.8 keV. In the experiment, sample 1 was first placed in an Al case, to the bottom of which the sample was attached with a tiny amount of soft adhesive agency (Goo, trade mark of Walthers, Milwaukee, WI 53218) to minimize effects of strain on the studied surface at the other end. Then the Al case was attached to a copper block. As for sample 2, however, the surface perpendicular to the observed one was directly attached to the copper block with Goo, because we assumed that the sample is large enough to relax strain. Each sample was mounted inside an beryllium can with helium gas to improve heat transfer and attached to the cold finger of a closed-cycle helium refrigerator. Both samples were oriented so as to have a [100] axis in the scattering plane. Although sample 2 was set to give a crystallographic ($hk0$) zone, the azimuthal angle of sample 1 was not determined.

In order to eliminate multiple scattering, we carried out energy scans at the forbidden reflections (100) between 5.0 and 8.0 keV and (300) between 6.5 and 8.0 keV above T_M. As shown in Fig. 2, multiple scattering appears as sharp peaks [typically ~ 5–10 eV FWHM and 10^4–10^5 counts per second (cps) compared with ~ 10^8 cps for (200)] at various incident energies. We looked for an energy range where intensity was low and constant, i.e., insensitive to a small energy variation. We finally decided to use the incident energy of 7.0 keV at (100) and 6.86 keV at (300) for sample 1 and 6.3 keV at (100) for sample 2 to study the new Bragg peaks. Intensities

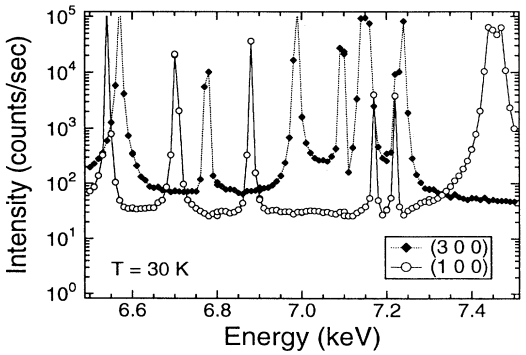

FIG. 2. Incident energy scans at 30 K at (100) and (300) of sample 1 after the etching. Similar scans before the etching show considerably broader peaks, overriding weak *new* Bragg peaks in entire energy range of the measurements.

shown in the figures of the present paper are normalized with monitor counts at a certain ring current of the synchrotron.

III. RESULTS

Figures 3 shows profiles of the fundamental Bragg peaks at various temperatures near T_M. In Fig. 3(a), sample 1 clearly shows a peak splitting corresponding to the tetragonal phase, though the tetragonal distortion is smaller ($c/a = 1.0014$) than the reported value [$c/a = 1.0024$ (Ref. 3)]. The peak profiles are fitted best with a single squared Lorentzian in a higher-temperature region and a double Gaussian at low temperatures, as indicated in Fig. 4. The intensity ratio of the two peaks in Fig. 3(a) corresponds to the domain distribution. Since the tetragonal phase has c domains having the (001) face and a domains having the (100) or (010) face, the ratio $I(001) : I(100) + I(010)$ should be 1 : 2 if the domain distribution is completely at random. Instead, Fig. 3(a) indicates that the ratio is 3 : 1. Unlike sample 1, sample 2 exhibits only the a domains as shown in Fig. 3(b). The tetragonal distortion is estimated at $c/a = 1.0025$, which agrees well with the reported value. We moved each sample perpendicular to the scattering plane to check the domain distribution at different positions. We, however, found no significant difference. Hastings *et al.*[10] reported that the etching gave rise to not only the reduction of the longitudinal peak width, but also the almost complete disappearance of the c domains. They speculated that *surface* damage leading to the strained surface was removed by the etching. Although we have confirmed the reduction of the longitudinal peak width as well as the mosaicity in sample 1 before and after the etching, we did not observe any significant change in the domain population.

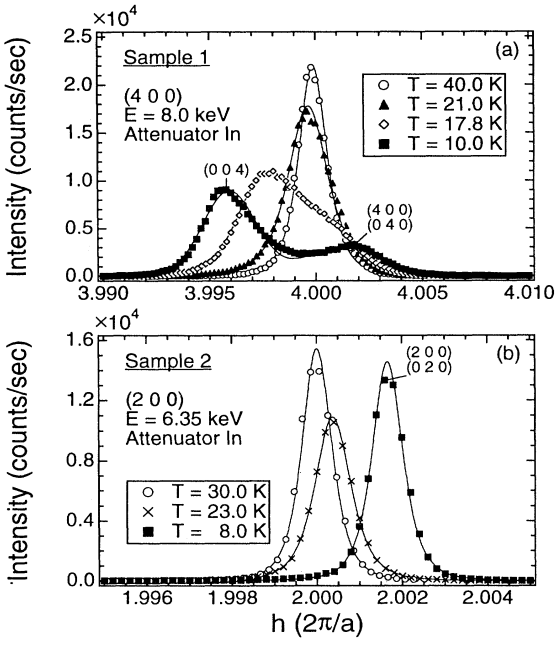

FIG. 3. Peak profiles of (a) the (400) reflection of sample 1 and (b) the (200) reflection of sample 2 at different temperatures around T_M. The peak profiles are fitted best with a single squared Lorentzian above T_M and a double Gaussian below T_M for sample 1, and a single squared Lorentzian for sample 2 at all measured temperatures. Fitting results are shown as solid lines.

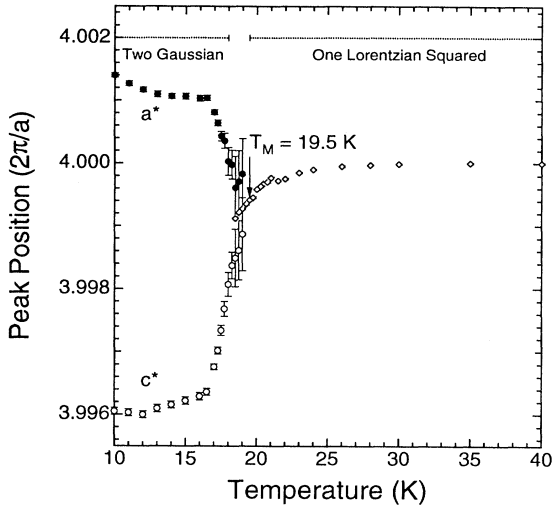

FIG. 4. Temperature dependence of the lattice parameter of sample 1. The tetragonal distortion $c/a = 1.0014$ is nearly half of the reported value 1.0024 in Ref. 7. Results of the single squared Lorentzian fitting above T_M are indicated with diamonds (◇). Results of the double Gaussian fitting below T_M are indicated with open circles (○) and solid circles (●). 4.0 in reciprocal lattice units (r.l.u.) $2\pi/a$ corresponds to $a = 4.718$ Å.

Figures 5 and 6 show the temperature dependence of the peak position, the width, and the intensity of the (100) reflection of sample 2, as well as several peak profiles. As indicated in Fig. 5(a), the lattice constant does not show a significant temperature dependence due to thermal expansion below 50 K. The peak position starts deviating from the constant value around 30 K; the directions of the deviation are different in two samples due to different domain distributions. On the other hand, as shown in Fig. 5(b), the peak width at (100) shows a small maximum at 23.7 K for sample 2 (19.5 K for sample 1), which corresponds to an inflection point in the curve of temperature dependence of the peak position. The peak splitting in sample 1 becomes apparent only below this temperature [see Figs. 3(a) and 4]. In accordance with Ref. 7, we extrapolate the curve and define $T_M = 19.5$ K for sample 1 and 25.0 K for sample 2. For convenience, we also introduce $T_I = 19.0$ K (sample 1) and 23.7 K (sample 2) for the inflection point to discuss the results.

As shown in Fig. 6, the new Bragg peaks at (100) and (300) appear only at the position corresponding to the a domain for both samples 1 and 2. Note that sample 1 consists of both a and c domains. These results exclude all but the $\Gamma_{12}(+)$-type displacement in four symmetry types compatible with the low-temperature tetragonal

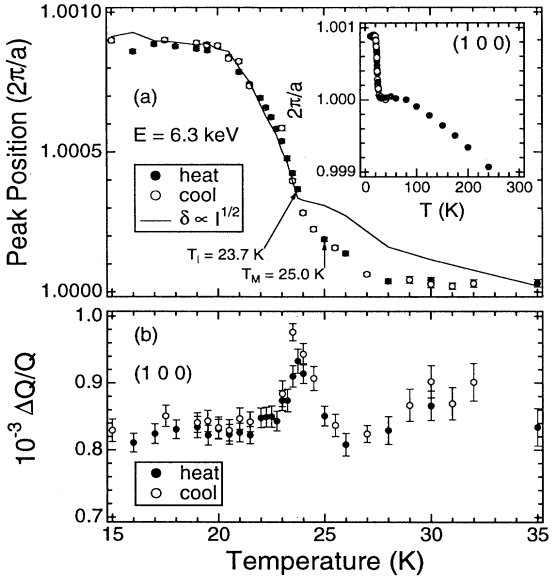

FIG. 5. (a) Temperature dependence of the (100) peak position of sample 2 on cooling and heating. The V-sublattice displacement δ estimated from the new Bragg peak intensity at (100) is indicated with a solid line, which scales the peak position perfectly below the inflection point T_I. 1.0 in r.l.u. $2\pi/a$ corresponds to $a = 4.718$ Å. (b) Temperature dependence of the (100) peak width $\Delta Q/Q$ of sample 2.

structure of V_3Si, which Perel, Batterman, and Blount proposed.[12] The atomic displacement is thus the same as that of Nb_3Sn, in which the structure factor is finite at (100) but vanishing at (001). In order to estimate the magnitude of sublattice displacements, we compared the intensity increase of the (100) forbidden reflection

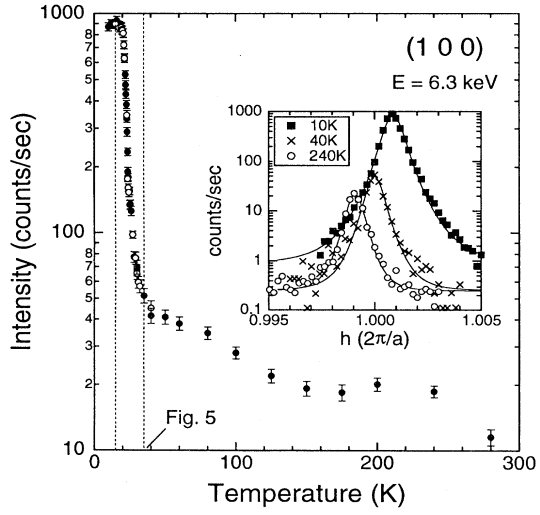

FIG. 6. Temperature dependence of the (100) intensity of sample 2 in logarithmic scale. The inset shows peak profiles at (100) at 10, 40, and 240 K.

below T_M, $\Delta I(100)$, with the intensity at (200) of sample 2. Since, in sample 2, all the reflections are given by the a domains, there is no ambiguity depending upon the domain distribution as discussed in Ref. 6. The ratio of the integrated intensities is $\Delta I(100)/I(200) = 5.6 \times 10^{-6}$. Taking into account appropriate Lorentz-polarization factors, the ratio of the structure factor is $\Delta F(100)/F(200) = 1.1 \times 10^{-3}$, which is converted to $\delta = 0.0011$ Å$(0.00024\,a)$. We also estimated δ by comparing the (300) and (400) reflections in the same way and obtained $\delta = 0.0015$ Å$(0.00031a)$. The displacement in Nb_3Sn was estimated at $\delta = 0.016$ Å$(0.0031\,a)$ in Ref. 6, which is an order of magnitude larger than that of V_3Si. Note that the estimated value is an upper limit for the displacement, since we do not consider extinction effects, which reduces the intensity of a strong reflection much more drastically than that of a weak one. We compared the integrated intensities at (400) and (420), whose ratio should be ideally $I(400)/I(420) = 6.6$. We estimated the ratio at 7.3, which is only 10% different from the calculated value. Thus, extinction effects are not dominant even if not completely negligible.

The solid line in Fig. 5(a) is the square root of the (100) intensity of sample 2, $\sqrt{I(100)}$, which scales the peak position below T_I almost perfectly. Since the atomic displacement δ is proportional to $\sqrt{I(100)}$ and the deviation of the (100) peak position can be converted to the tetragonal strain $(c/a - 1)$, this establishes that the internal sublattice displacements are linear to the spontaneous tetragonal strain, as already known for Nb_3Sn.[6] Above T_I up to 30 K, however, δ does not scale the peak position very well. As for sample 1, its normalized (100) intensity at 10 K is about 20 times smaller than that of sample 2. This difference can be ascribed to fewer ($\sim 1/4$) a domains and smaller ($\sim 1/2$) tetragonal distortion in sample 1 than in sample 2 because the intensity is proportional to the domain population times square of the tetragonal distortion. Note that all the dependences show no observable thermal hysteresis and indicate a rather continuous transition. A thermal expansion study on V_3Si, however, has clarified that the thermal expansion coefficient along [100] shows discontinuity accompanied by a volume change at T_M.[19] Therefore, the transformation must be weakly first order, as proposed by theory.[20]

In the course of establishing the order parameter, we unexpectedly found that there remain finite intensities at (100) and (300) well above T_M, which intensities are considerably larger than the background intensity of about 0.1 cps. This *residual* intensity gradually increases with decreasing temperature in a wide temperature range between room temperature and T_M, as shown in Fig. 6 for sample 2. The quantitatively similar temperature dependence is seen in sample 1. At each temperature, the sample was carefully lined up to make sure that the intensity was always maximized. As indicated in the inset of Fig. 6 showing peak profiles of the (100) reflection at different temperatures, the peak width does not show any significant temperature dependence between room temperature and 30 K and is always resolution limited. We also performed incident energy scans at (100) at differ-

ent temperatures. The constant region ranging over 100–200 eV around the studied energy position increases as a whole with decreasing temperature for both samples. Moreover, incident energy scans in a wide range show that the positions of multiple-scattering peaks shift no more than 10 eV between room temperature and 10 K. These results exclude the possibility that the temperature dependence of the (100) reflection is merely due to contamination from a tail of a multiple-scattering peak shifting with temperature. Another conceivable extrinsic reason is extinction release. This effect, however, is also excluded because it should be much more apparent in the strong fundamental reflections, which did not show any such behavior in the present study. Moreover, weak reflections are seldom affected by this effect. We, therefore, believe that the temperature dependence of the residual intensity at the forbidden (100) reflection is intrinsic and most likely a precursor to the martensitic transition.

Figure 7 shows temperature dependence of the (300) peak profile and the intensity for sample 1. The peak profiles are almost perfectly fitted with a single squared Lorentzian above T_M and with a double Gaussian below T_M. There clearly exists a single peak at the cubic position above T_M, which corresponds to the residual intensity seen at (100). Below T_M, the new Bragg peak appears only in the a domain, i.e., at (300) and (030), while the residual intensity stays at almost the same position and shows a small peak in the intensity at T_M. The new Bragg peak, separated from the residual intensity, scales very well the tetragonal strain up to T_M, as indicated with the solid line. The residual intensity exhibits a broadening in the width below T_M, indicating effects from the tetragonal distortion. These results clearly reveal that the new Bragg peak and the residual intensity are different entities. Since sample 2 has much larger intensity for the new Bragg peak, it is practically impossible to resolve the (300) peak below T_M in two parts.

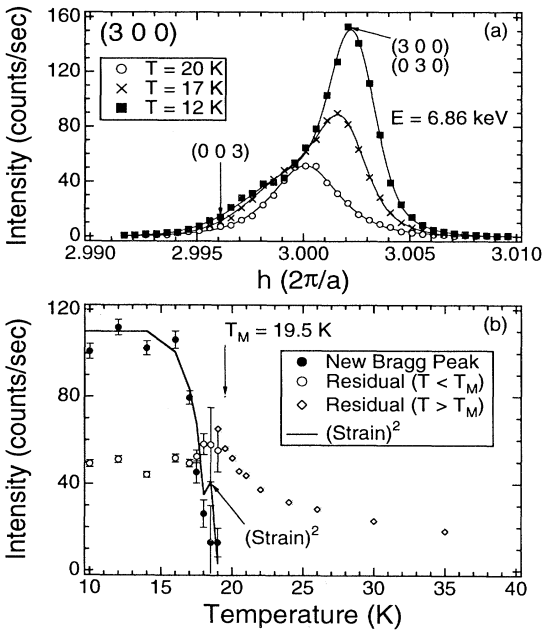

FIG. 7. (a) Peak profiles of the (300) reflection of sample 1 near T_M. The peak profiles are fitted best with a single squared Lorentzian above T_M and a double Gaussian below T_M, as shown as solid lines. (b) Temperature dependence of the intensities obtained from the fitting. The solid line indicates square of the estimated tetragonal strain $(c/a-1)$. Results of the single squared Lorentzian fitting above T_M are indicated with diamonds (◇). Results of the double Gaussian fitting below T_M are indicated with open circles (○) and solid circles (●), corresponding to the residual intensity and the new Bragg peak, respectively.

IV. DISCUSSION

As mentioned in the previous sections, sample-dependent properties of V_3Si have been reported by several authors. These studies can be summarized as follows: (i) T_M linearly scales the resistivity ratio $\rho_{300\ K}/\rho_{18\ K}$, which corresponds to the inverse of defect concentration.[7,8] (ii) Broadening of the martensitic transition can probably be ascribed to an existence of the second phase,[7] an inhomogeneity of the samples,[8] or surface strain.[9,10] According to a theory,[20] a sufficient $\langle 001 \rangle$ stress would suppress a small cubic term leading to the weak first order in the free energy and leave a smooth variation of the distortion with temperature. (iii) In addition, Ott, Chandrasekhar, and Seeber[19] pointed out that a crystal stressed uniaxially shows the a axis lined up parallel to that direction, giving rise to the domain distribution different from an unstressed sample. With these backgrounds, we can conclude that sample 2 is a *well-behaved* sample, but receiving a stress probably due to a direct adhesion causing the rather broad transition and the biased domain distribution, and that sample 1 is not as well behaved as sample 2 whereas showing less effects of stress.

Besides the (100) and (300) forbidden reflections reported here, other forbidden reflections were previously measured by Borie,[14] and Schmidt and Colella,[15,16] inspired by a theoretical prediction by Borie.[13] Using symmetry considerations to analyze the allowed moments up to third order for V and Si atoms in V_3Si, Borie pointed out that two types of forbidden reflections might be thermally excited for the V atoms, namely, (i) type A (h,k,l all odd), due to only anharmonicity (non-Gaussian atomic distribution), and (ii) type B (h odd; $k,l=4n$ or $k,l=4n+2$), arising from anisotropic atomic motion and anharmonicity. Note that a reflection having same numbers in two indices vanishes in both types. As shown in Fig. 8, Schmidt and Colella[16] reported the temperature dependence of the forbidden reflections at (140) in type B (mostly due to anisotropic atomic motion) and at (153) in type A with using x rays from a rotating anode. They reported that, for the nontransforming crystal, the (140) structure factor $F(140)$ at room temperature is estimated at -0.325 electrons and that $F(153)$ at 22 K is equal to -0.067 electrons.[15] Our result of the (100) reflection of sample 1 is also shown in Fig. 8 for comparison. The temperature dependence of the (140) reflection suggests

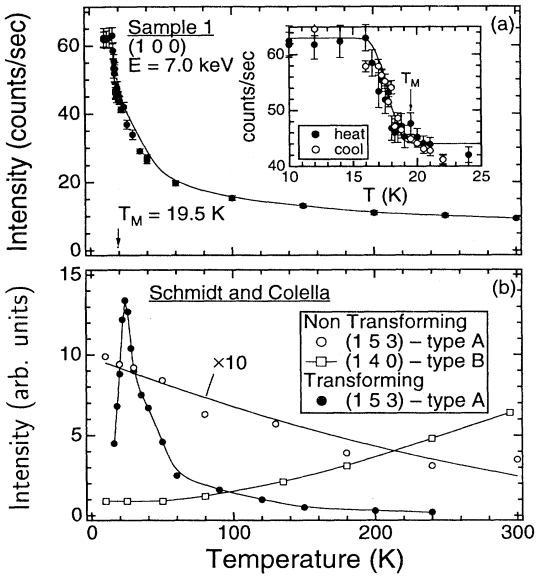

FIG. 8. (a) Temperature dependence of the (100) reflection of sample 1. (b) Temperature dependence of the (153) type-A and (140) type-B reflections after Ref. 16.

that the difference between displacements parallel and perpendicular to the V chain increases with increasing temperature. On the contrary, the (153) reflection shows the opposite temperature dependence, indicating the increase of the anharmonicity with *decreasing* temperature. Similar temperature dependence is seen in the (100) reflection of sample 1. Schmidt and Colella found that the (153) reflection of the transforming crystal is more intense at low temperatures than the nontransforming one and shows a peak at 25.2 K, where $F(153)$ reaches about -0.3 according to Fig. 3 in Ref. 16. They, however, concluded that the anharmonicity peaking is not directly correlated with the martensitic transformation because that temperature is well above the maximum of T_M (20.5 K) reported for a series of samples in Ref. 8. As we have shown in Sec. III, however, T_M can go up to 25 K or more. Since Schmidt and Colella noted that they did not monitor allowed reflections at different temperatures to determine T_M because of experimental restrictions, it is possible that 25.2 K matches T_M of their sample and that the temperature dependence of the (153) reflection is relevant to the martensitic transition.

This increase of the anharmonicity towards T_M is understood in the framework of the soft-mode phonon theory and neutron-scattering experiments.[11] Moreover, by x-ray scattering, Staudenmann and Testradi[21] reported very large second and fourth moments for the mean position distribution of the V atoms at 78 K. No such unusual behavior was found at room temperature. These observed moments, much larger than expected for a harmonic lattice, were interpreted as evidence for localization of V atoms at off-lattice sites, giving rise to large anharmonicity. Their observation prompted Yu and Anderson[23] to develop a model in which strong electron-phonon coupling leads to anharmonic phonons and an effective double-well potential for each metal atom. It is naturally expected that lowering the temperature would cause the atom to localize in one of the double-well minima, 0.1–0.2 Å off the lattice site, and eventually cause a large displacive transition. The actual lattice displacement is, however, much smaller. Yu and Anderson found that, as the temperature decreases, the hopping fugacity increases and the double well becomes shallower, thus confronting the tendency of localization and preventing a transition from occurring. Their finding can explain that the martensitic transition in V_3Si has such small lattice displacements and occurs at such low temperature though there are phonon anharmonicities from much higher temperatures. However, an extensive energy-dispersive x-ray-diffraction study in a wider Q range (up to $\sim$ 30 Å^{-1}, compared to $\sim$ 17 Å^{-1} in Ref. 21) by Tranquada, Trautmann, and Heald[22] indicates that the non-Gaussian part of the V distribution is significantly smaller than the result of Staudenmann and Testradi,[21] while they also have confirmed that anharmonicity at the V sites increases with decreasing temperature.

Although the localization of V atoms at off-lattice sites above T_M appears inconclusive, anharmonic phonon behaviors at low temperatures have been established by x-ray- as well as neutron-scattering measurements. Thus, the results for (153) can be interpreted as anharmonicity increasing towards the martensitic transition. Figure 7(b) indicates that the residual intensity at (300) separated from the new Bragg peak in sample 1 shows a small peak at T_M. Because of uncertainty in the fitting, it is not definite whether the peak corresponds to the clear peaking at (153) in Ref. 16. Note that the anharmonicity effect becomes clearer with increasing the Q vector. Thus it is natural that we see stronger anharmonicity effects at (153) than at (100) and (300). Comparison of the structure factors above T_M indeed reveals $F(300)/F(100) =$ 3.1–3.8, suggesting that the residual peak has a phonon-like Q dependence. The theory by Borie,[13] however, is not directly applicable to our observation because the (100) and (300) reflections do not belong to either type A or B in the theory.

Another possible intrinsic reason for the residual intensities is a covalency effect, which was reported in diamond in 1921.[24] Trucano and Batterman[17] measured the forbidden (442) reflection of Si between 20 and 500 °C and found that $F(442)$ decreases to zero at 250 °C and then increases to almost twice its room temperature value at 500 °C. They concluded that this temperature dependence is consistent with contributions to the structure factor from both the asymmetric bond distribution F_{bond} and anharmonic thermal atomic motion F_{anh}. They showed that F_{anh} increases with temperature and cancels F_{bond}, which is of opposite sign and much less temperature dependence, at about 250 °C producing zero intensity. It is also possible to think an asymmetric bond electron distribution for V in V_3Si to result in the (100) reflection. Since we have already calculated the structure factor at (100) of sample 2, we can estimate the number of bonding electrons between V atoms. Assume that all the residual intensity at (100) is due to the asymmetric

bond electron distribution, we find that $|F_{\text{bond}}|$ is 0.012 electrons at 100 K and reaches 0.019 at 30 K and 0.028 electrons at $T_M = 25$ K. This implies that the (100) residual intensity is an order of magnitude or two smaller than other type of forbidden reflections at (140) and (153). It is thus indispensable to utilize intense synchrotron radiation to observe the (100) and (300) residual peaks. Although it is very attractive to speculate that the electron distribution around V anticipates the martensitic transition at low temperature, the present work itself has no direct experimental evidence to support the idea.

The electron charge distribution in V_3Si at 300 and 13.5 K has been reported by Staudenmann *et al.* by x-ray-diffraction measurements.[18] They measured approximately 2000 reflections from a spherical specimen of ~ 0.1 mm and performed a Fourier transformation to obtain the valence and deformation densities after subtraction of the appropriate atomic density functions. They assumed the $Pm\bar{3}n$ cubic space group through the analysis. They found that a pair of anisotropic rings, which do not exist at 300 K, appears around every second V-V bond at 13.5 K. Each of two rings is on a plane perpendicular to the V chain. As a result, the electron density between two consecutive V atoms becomes larger and smaller alternatively along a V chain at 13.5 K, compared to that at 300 K. This is qualitatively consistent with our observation. Since their measurements in Ref. 18 were limited to two temperatures, we cannot make further comparison. Although their measurements and analyses appear careful and accurate, they, by some means, overlooked contaminations due to multiple scattering, which may completely alter the intensities of many reflections, thus the density map, eventually.

To summarize, in addition to establishing the order parameter in the martensitic transition of V_3Si, we found that there remain residual intensities at (100) and (300), which are supposed to be forbidden above T_M. We believe that this phenomenon is a precursor to the martensitic transition, possibly due to either the anharmonicity in the softening of the zone-center phonon or the covalency effect between the V atoms. For a more complete understanding, it is necessary to perform a definitive study of (003) and (300) below T_M in the first place. This investigation will allow us to separate the new Bragg peak from the residual intensity at (003). We also plan to extend our measurement to not only the (153) but also to other types of forbidden reflections. On the basis of these extensive observations, we hope to construct an appropriate explanation of the appearance of these forbidden reflections.

ACKNOWLEDGMENTS

The authors are deeply indebted to Doon Gibbs for his advice and support during the experiments and S. J. Williamson for providing several samples including sample 1. We are also pleased to acknowledge stimulating discussions with J. B. Hastings, J. L. Staudenmann, and J. M. Tranquada. One of the authors (K.H.) also wishes to thank D. E. Cox and A. C. Langhorn for their help for etching the crystals using hydrofluoric acid. Work performed in the Brookhaven Physics Department was supported by the Division of Materials Research, U.S. Department of Energy under Contract No. DE-AC02-76CH00016.

* Present address: WPI Group, 5 East 57th Street, New York, NY 10092.

[1] L. R. Testradi, Rev. Mod. Phys. **47**, 637 (1975).
[2] B. W. Batterman and C. S. Barrett, Phys. Rev. Lett. **13**, 390 (1964).
[3] R. Mailfert, B. W. Batterman, and J. J. Hanak, Phys. Lett. **24A**, 315 (1967); Phys. Status Solidi **32**, K67 (1969).
[4] G. Shirane and J. D. Axe, Phys. Rev. Lett. **27**, 1803 (1971).
[5] J. D. Axe and G. Shirane, Phys. Rev. B **8**, 1965 (1973).
[6] G. Shirane and J. D. Axe, Phys. Rev. B **4**, 2957 (1971).
[7] B. W. Batterman and C. S. Barrett, Phys. Rev. **145**, 296 (1966).
[8] M. N. Khlopkin, JETP Lett. **39**, 358 (1984).
[9] J. B. Hastings, G. Shirane, and S. J. Williamson, Phys. Rev. Lett. **43**, 1249 (1979).
[10] J. B. Hastings, Y. Fujii, G. Shirane, and S. J. Williamson, Phys. Rev. B **28**, 322 (1983).
[11] G. Shirane, J. D. Axe, and R. J. Birgeneau, Solid State Commun. **9**, 397 (1971).
[12] J. Perel, B. W. Batterman, and E. I. Blount, Phys. Rev. **166**, 616 (1968).
[13] B. Borie, Acta Crystallogr. A **30**, 337 (1974).
[14] B. Borie, Acta Crystallogr. A **37**, 238 (1981).
[15] M. C. Schmidt and R. Colella, Phys. Rev. Lett. **55**, 715 (1985).
[16] M. C. Schmidt and R. Colella, Phys. Rev. B **34**, 2872 (1986).
[17] P. Trucano and B. W. Batterman, Phys. Rev. B **6**, 3659 (1972).
[18] J. L. Staudenmann, P. Coppens, and J. Muller, Solid State Commun. **19**, 29 (1976); J. L. Staudenmann, *ibid.* **23**, 121 (1977); **26**, 461 (1978).
[19] H. R. Ott, B. S. Chandrasekhar, and B. Seeber, Phys. Rev. B **31**, 2700 (1985).
[20] R. N. Bhatt and W. L. McMillan, Phys. Rev. B **14**, 1007 (1976).
[21] J. L. Staudenmann and L. R. Testradi, Phys. Rev. Lett. **43**, 40 (1979).
[22] J. M. Tranquada, C. Trautmann, and S. M. Heald, Phys. Rev. B **35**, 4193 (1987).
[23] Clare C. Yu and P. W. Anderson, Phys. Rev. B **29**, 6165 (1984).
[24] W. H. Bragg, Proc. Phys. Soc. London **33**, 304 (1921).